Usage guidelines

Please refer to the usage guidelines at http://sure.sunderland.ac.uk/policies.html or alternatively contact sure@sunderland.ac.uk.

The Staining Pattern of Brilliant Blue G During Macular Hole Surgery: A Clinicopathologic Study

David H. W. Steel,[1,2] Christiana Dinah,[1] Haifa Magdi,[1] Kathryn White,[3] and Jon Rees[4]

[1]Sunderland Eye Infirmary, Sunderland, United Kingdom
[2]Institute of Genetic Medicine, Newcastle University, Newcastle Upon Tyne, United Kingdom
[3]EM Research Services, Newcastle University, Newcastle Upon Tyne, United Kingdom
[4]Faculty of Applied Sciences, University of Sunderland, Sunderland, United Kingdom

PURPOSE. To describe the intraoperative staining pattern of the internal limiting membrane (ILM)-specific dye Brilliant Blue G (BBG) in a cohort of patients with idiopathic macular holes; to analyze the associations of the staining pattern with pre- and postoperative variables and to correlate the staining pattern with transmission electron microscopy (TEM) of the excised ILM.

METHODS. Fifty-five consecutive patients were studied. The staining pattern was divided into three subtypes based on the intraoperative appearance. The presence of a narrow rim of nonstaining around the macular hole (MH) edge was noted and measured. In the final 21 patients, the excised ILM was examined with TEM.

RESULTS. The pattern of staining observed was categorized as uniform in 33 patients (60%), patchy nonstaining in 17 (31%), and no visible staining in 5 (9%). The staining pattern correlated with the MH stage. In the patients with uniform or patchy staining, a nonstaining rim was observed in 26 (52%) of the 50. The presence of a rim was associated with a greater hole diameter and lower postoperative visual acuity. The stain pattern correlated significantly with the amount of cellular tissue on the vitreous side of the ILM on TEM, with a greater proportion of multicellular layer membranes and new collagen in the incomplete staining groups.

CONCLUSIONS. A variety of nonstaining patterns around macular holes can be observed using BBG, and these patterns correlate to the amount of cellular tissue on the vitreous side of the ILM seen histologically. These patterns could be used to guide the ILM peeling requirement or extent in future studies.

Keywords: Brilliant Blue G, staining, internal limiting membrane, macular hole, vitrectomy, electron microscopy

Peeling of the internal limiting membrane (ILM) has been shown to improve the success rate of macular hole (MH) surgery.[1] It is thought to improve hole closure by ensuring the release of tangential traction on the edges of the hole from the ILM itself, which contributes significantly to the biomechanical strength of the retina, and also by removing all vitreous and cellular debris from around the MH after vitreo-retinal separation, which could exert persistent tractional effects.

Brilliant Blue G (BBG) is a relatively new ILM stain and is being widely adopted by surgeons because of its selective ILM staining properties and low toxicity.[2–5] Related to its specificity of stain, areas of nonstaining by BBG can be used to demonstrate putative areas of residual vitreous cortex and cellular proliferation on the ILM in the same way as Indocyanine Green (ICG) staining.[2–7] Several authors have observed these effects in MH patients undergoing surgery, but their patterns and occurrence have not been systematically described or their associations with any pre- or postoperative variables examined.[8,9] Furthermore, the histopathologic correlation of the staining patterns has not been studied.

In this report, we describe the staining pattern of BBG in a consecutive cohort of patients with idiopathic macular holes

undergoing ILM peeling and analyze the associations of the staining patterns with various pre-, intra-, and postoperative variables including retinal hemorrhages that occurred at the time of surgery. In a subset of the patients, we examined the removed ILM with transmission electron microscopy (TEM) and related the findings to the observed staining patterns.

METHODS

Consecutive patients undergoing surgery by one surgeon for idiopathic macular holes over a 2-year period were included in the study. The study followed the tenets of the Declaration of Helsinki, with approval from the local institutional review board. Informed consent was obtained from the subjects after explanation of the nature of the study. Patients with traumatic macular holes, high myopia (>6 diopters), or previous retinal surgery were excluded from the study. Patients with less than 3 months follow-up were also excluded. All patients underwent transconjunctival 25-gauge (25-g) vitrectomy using wide-field noncontact viewing (Eibos, Haag-Streit, Switzerland) with combined phacoemulsification and intraocular lens (IOL) implantation if phakic. Patients with vitreous separation from
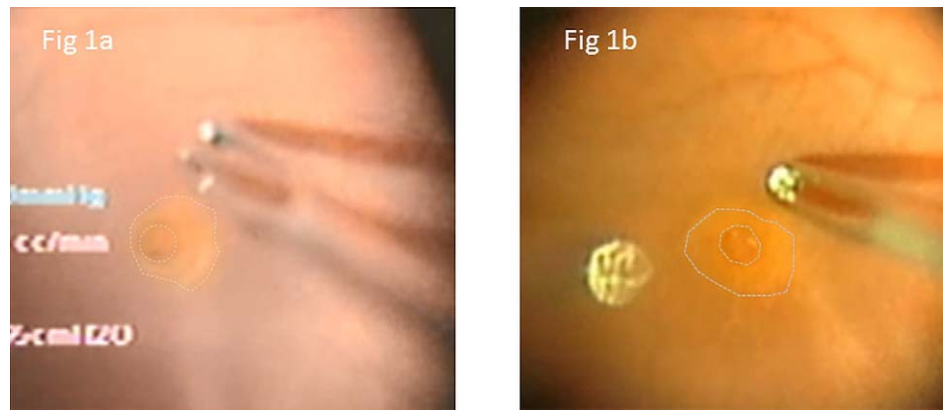
FIGURE 1. (**a**, **b**) Examples of a rim of nonstaining around otherwise uniformly stained cases. Macular hole margin and edge of rim of nonstaining are highlighted by *dashed lines*. The *bright circular area* to the *left* of the hole in (**b**) is an artifact.

the optic disc head with a visible Weiss ring were recorded. In other cases, posterior hyaloid face separation was achieved with aspiration. In cases of stage 4 holes with apparent vitreous separation already present, the presence of residual vitreous was checked for with diluted triamcinolone staining.

ILM Staining and Peeling Procedure

Brilliant Blue G (ILM Blue; Dorc International, Zuidland, The Netherlands) was used to stain the macula in all cases. This is a highly purified preparation of 0.025% BBG mixed with 4% polyethylene glycol to produce a heavier-than-water solution, with a density of 1.01 kg/L. The technique of staining was to aspirate approximately 0.2 mL undiluted BBG into the vitrectomy probe and then reflux the undiluted BBG over the macular via the vitrectomy probe, using the proportional reflux function of the vitrectomy machine (Constellation; Alcon, Fort Worth, TX, USA). Due to the heavier-than-water density of the dye solution, it sinks to the macular retina. We used valved sclerostomy ports and thus the infusion was kept on during the staining. After 5 seconds, the dye was removed with aspiration, again using the vitrectomy probe, until the vitreous cavity was clear. A macular contact lens was used to view the peeling procedure. The ILM was peeled using a pinch technique and Grieshaber DSP 25-g end-gripping forceps (Schaffhausen, Switzerland) and a peel radius of approximately one disc diameter. In cases in which there was incomplete staining of the ILM with adherent pre-ILM tissue, an area of ILM that had normal staining was selected and the peel initiated from there. The pre-ILM tissue and ILM were hence peeled en bloc, without the need for a second peel. All surgeries were video recorded for later analysis of the staining pattern and characteristics.

Either 25% SF6 or 20% C2F6 gas was used as a tamponade agent, and the patients were instructed to position facedown for 3 days. Patients were reviewed at 2 weeks and 3 months postoperatively. Pre- and postoperative best-corrected visual acuity (BCVA) at 3 months was measured using a standard Snellen acuity chart and converted to logMAR scores for the purposes of statistical analysis.

Intraoperative video recordings were used to analyze the staining pattern of the BBG prior to peeling. It was noted that in many cases there was a rim of nonstaining around the MH edge (Fig. 1). This was measured in four meridians from the video still images (using the known MH size in each case), and an average width was calculated. The staining pattern around the rest of the central macula was then graded. The staining pattern was divided into three subtypes (Fig. 2).

1. A uniform staining pattern with the ILM homogenously stained across the macula;
2. A patchy staining pattern with localized areas of nonstaining randomly oriented around the macula; and
3. Absence or near absence of any identifiable staining for at least a 1200-μm radius around the foveal center.

Patients underwent spectral-domain optical coherence tomography (SD-OCT) on the Heidelberg Spectralis (Heidelberg Engineering, Heidelberg, Germany) immediately preoperatively and 3 months postoperatively to assess closure. Preoperatively the minimum linear diameter (MLD) of the hole was measured as previously described using the Spectralis measuring tools.[10] The presence or absence of vitreous attachment to the MH rim was recorded. The holes were classified as stage 2 to 4 based on the Gass classification, with a MLD of 400 μm being used to divide stage 2 from stage 3 holes and a stage 4 hole defined by the presence of a complete posterior vitreous detachment, with a Weiss ring observed clinically, regardless of hole dimensions.[11]

Holes were considered closed, indicating anatomical success, if there was complete circumferential hole rim reattachment without a full-thickness foveal neurosensory retinal defect demonstrated on OCT.

Transmission Electron Microscopy

The ILM from the final 21 consecutive patients was placed and fixed immediately in 2% glutaraldehyde in 0.1 M sodium cacodylate buffer. The ILM was enrobed in low-melting-point agarose (4%) to form a small block (this made the ILM easier to handle). After secondary fixation in 2% osmium tetroxide, the samples were dehydrated in graded acetone, embedded in epoxy resin, and polymerized at 60°C. Ultrathin sections (70 nm) were taken at two levels through the block, stained with uranyl acetate and lead citrate, and viewed on a Philips CM100 transmission electron microscope (Philips/FEI Corp., Eindhoven, Holland).

For estimation of the amount of cellular tissue on the vitreous or retinal side on the ILM, images were taken at ×7900 magnification from 14 randomly sampled areas of the ILM. To quantify the amount of debris on each surface of the ILM, a grid of lines (line length 2 μm) was superimposed on each image. The number of intercepts between the grid line and retinal or vitreous surface was counted. Another grid (line length 1 μm) was then superimposed on each image, and the number of intercepts between the grid lines and any retinal- or vitreous-side tissue was counted. The percentage of surface covered by
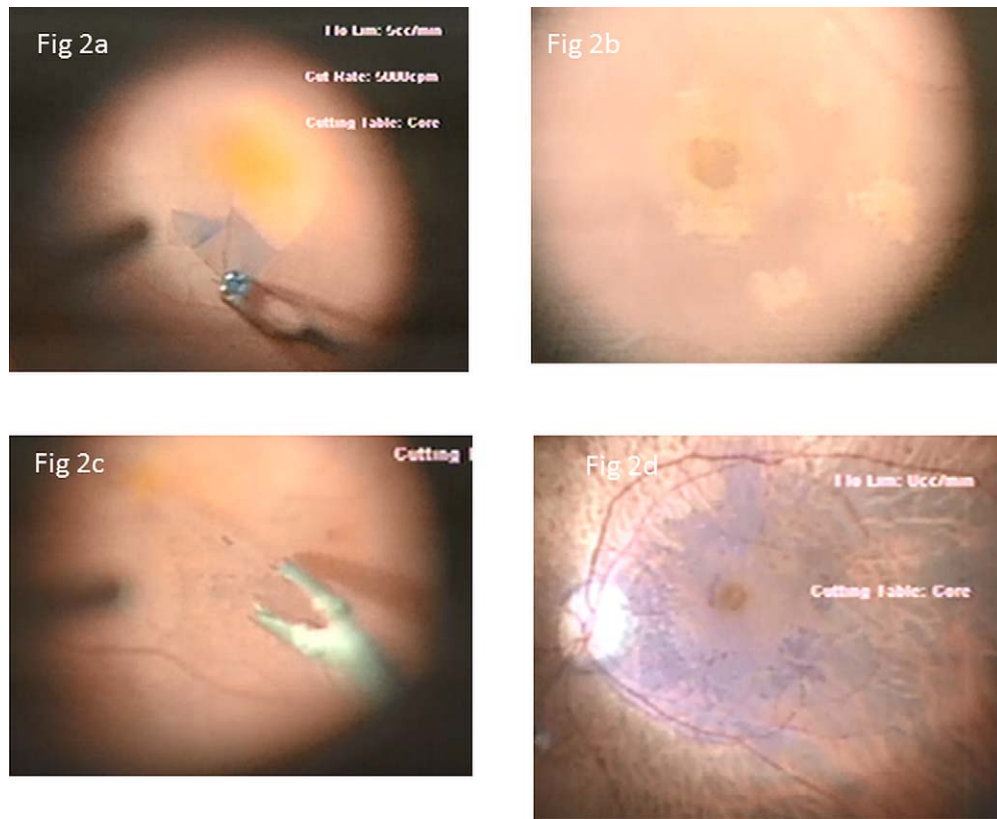
FIGURE 2. (**a–d**) Example of staining patterns observed. (**a**) A uniformly stained ILM best appreciated during peeling. (**b**) A case with patchy nonstaining before peeling and (**c**) with stippled patchy staining best shown during peeling. (**d**) A case of a large zone on nonstaining around the hole.

cellular tissue was taken as the number of intercepts on tissue / (number of intercepts on the ILM surface × 2) × 100 (Fig. 3).

More detailed examination of the vitreous-side tissue was then performed to determine whether there were any areas of collagen and whether this collagen was native or newly formed, and the cellular pattern of the tissue was observed.

In three patients with uniform staining but a visible nonstaining rim, the ILM was peeled and kept as two separate
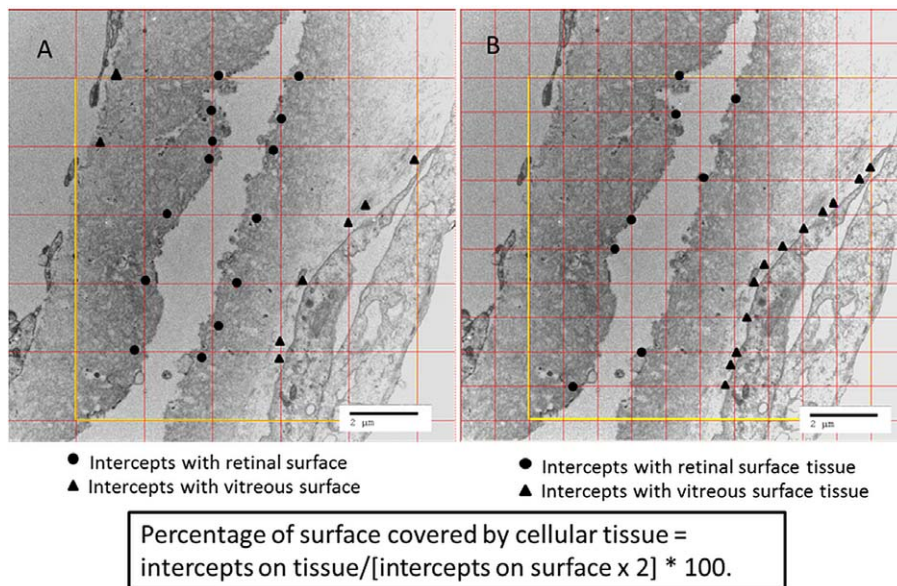

Percentage of surface covered by cellular tissue =
intercepts on tissue/[intercepts on surface x 2] * 100.

FIGURE 3. Method used to estimate extent of ILM surface tissue.

specimens—the first comprising the rim only and the second the surrounding ILM.

Statistical Analysis

Descriptive and statistical analysis was performed using IBM SPSS Statistics 21 (IBM, White Plains, NY, USA). Patients' demographic characteristics, pre- and postoperative variables, and MH features are presented in terms of mean, standard deviation and range or percentage as appropriate.

For analysis, the patchy and nonstaining cases were grouped together and compared to the uniform staining group. Two-sample *t*-tests were used to compare continuous variables. Relationships between continuous variables were evaluated using Pearson's correlation coefficient, and associations between noncontinuous variables were analyzed via the χ^2 statistic using Fisher's exact probability because of small numbers. Percentage of ILM sections with retinal- or vitreous-side tissue between the three staining groups and between Gass stages was compared using independent measures ANOVA with Tukey post hoc testing. Statistical significance was considered with a *P* value of 0.05 or less.

RESULTS

The study period was from January 2012 to September 2013. During the study period, 56 patients were included. One patient was excluded because of incomplete follow-up (patient died of myocardial infarction 2 months postoperatively), leaving 55 patients' data to be analyzed. No patient had bilateral surgery.

Forty-one patients were female (75%), and the mean age was 70.5 years (range, 53–86 years). The mean preoperative vision was logMAR 1.04 (standard deviation [SD] 0.36).

Holes were classified as stage 4 in 9 cases (17%), stage 3 in 21 (38%), and stage 2 in 25 (45%).

Seventeen patients were pseudophakic (31%), and the rest had combined surgery with phacoemulsification and IOL. C2F6 gas was used in 20 patients (36%) and SF6 in the others.

Vitreous was visibly attached to the MH rim on the OCT preoperatively in 21 patients (38%). Hole closure was achieved in 53 patients (96%).

The preoperative characteristics are summarized in Table 1.

Staining Pattern

The overall pattern of staining observed in the macular area was categorized as uniform in 33 cases (60%), patchy nonstaining in 17 (31%), and no visible staining in 5 (9%). The pre- and postoperative variables divided by staining pattern group are shown in Table 2.

There were significantly more patients with stage 2 holes with a uniform pattern of staining and more patients with stage 4 holes with a patchy or nonstaining pattern (*P* = 0.001).

Excluding the cases with an overall nonstaining pattern, a nonstaining rim was observed intraoperatively in 26 of the 50 patients (52%). The rim size in any one meridian ranged from 75 to 700 μm with a mean of 291.62 μm (SD 156.61; range, 75–575).

The presence of a nonstaining rim was more frequently seen in cases with incomplete staining than in those with uniform staining. There were 13 patients in each of the uniform and patchy staining groups (39% and 76%, respectively) with a rim, compared to 20 (61%) in the uniform group and 4 (24%) in the patchy group without a rim (*P* = 0.02).

There was a significant difference in MLD between those patients with a rim and those without, and the postoperative

TABLE 1. Summary of Patient Characteristics

Variables	Values
Age, y, mean (SD)	70.52 (7.06)
Sex, *n* (%)	41 female (75), 14 male (25)
Gass stages 2, 3, 4, *n* (%)	25 (45), 21 (38), 9 (17)
Minimum linear diameter, μm, mean (SD)	380.40 (192.19)
Base diameter, mean (SD)	758.56 (399.15)
Phakic/pseudophakic, *n* (%)	38 (69)/17 (31)
SF6 gas/C2F6 gas, *n* (%)	35 (64)/20 (36)
Number of intraoperative superficial retinal hemorrhages in peel area, median (range)	1 (1–11)
Preoperative Va, logMAR, mean (SD)	1.04 (0.36)
Postoperative Va, logMAR, mean (SD)	0.38 (0.24)

Va, visual acuity.

visual acuity was significantly worse in the group with a nonstaining rim (Table 3).

In the 26 patients with a discrete measurable nonstaining rim (excluding the nonstaining group), there was a strong and statistically significant relationship between the average rim width in an individual patient and the MH width ($r = 0.635$, $P = 0.0002$).

Electron Microscopy

Vitreous-side tissue was apparent as combinations of native vitreous collagen, typically present between the ILM and any cellular component, newly formed collagen usually mixed in with cellular membranes, and single cells and mono- and multilayers of cells (Fig. 4). Similarly, retinal-side tissue could be classified as small fragments (less than 2 μm in size), larger fragments of parts of cells with identifiable intracellular organelles, and more complete layers of cells (Fig. 5). The nature of the vitreous- and retinal-side tissue observed between those with a patchy and those with a nonstaining pattern was not significantly different; these are presented as one group and contrasted to those with a uniform pattern (Table 4). Mono- and multilayers of cells and newly formed collagen were observed more frequently in the incomplete staining groups.

The percentage area of the ILM covered by vitreous tissue varied widely from 0.3% to 76% (mean 25.2%, SD 27.6). There was significantly less vitreous surface tissue on the ILM in patients with a uniform staining pattern than in those with an incomplete pattern ($P < 0.001$), but there was no significant difference between the patchy nonstaining and the nonstaining group (Table 5).

There were no significant differences between the three staining groups in terms of retinal-side tissue, and no significant correlation was found between the percentage of vitreous-side tissue and percentage of retinal-side tissue ($r = 0.148$, $P = 0.523$).

In the 21 ILM specimens studied, there were 5 from stage 2 holes, 10 from stage 3 holes, and 6 from stage 4 holes. There was a significant difference in the percentage of vitreous-side tissue present between the three stages of MH. The mean percentage of vitreous-side tissue was 7.4%, 19.9%, and 48.9% in the stage 2, 3, and 4 groups, respectively ($P = 0.029$).

There was not a significant association between the number of retinal hemorrhages and the percentage of retinal-side tissue present ($r = 0.298$, $P = 0.189$).

TABLE 2. Patient Characteristics Between the Three Staining Patterns Observed

	Uniform, $n = 33$	Patchy, $n = 17$	Nonstaining, $n = 5$	P^*
Age, y, mean	69.55	71.18	74.80	0.210
Female sex (%)	25 (76)	14 (82)	2 (67)	0.999
Stages 2, 3, 4 (%)	19, 13, 1 (35, 23, 2)	4, 7, 6 (7, 12, 11)	2, 1, 2 (4, 2, 4)	0.001
Minimum linear diameter, μm, mean	357.67	461.12	256.00	0.287
Vitreous attachment present, %	16	5	0	0.088
Occurrence of petechial retinal hemorrhages in peel area, mean	1.52	2.00	0.40	0.336
Preoperative Va, logMAR, mean	1.06	1.04	0.940	0.771
Postoperative Va, logMAR, mean	0.342	0.513	0.220	0.223
Nonclosure, n	1	1	0	0.999

* The data were analyzed with the patchy and nonstaining cases in one group as described in the statistical analysis section.

The findings from the three patients in whom the rim ILM was analyzed separately from the rest of the ILM specimen are presented in Table 6. No vitreous collagen was found on the specimens, and the vitreous cellular tissue was a monolayer in two patients and near-confluent single-cell clusters in the remaining one.

DISCUSSION

Inner limiting membrane peeling is thought to improve MH closure by reducing the tangential traction present after vitreous separation below that needed for hole closure. This tractional force is in part related to the amount of residual vitreous cortex and cellular material remaining on the ILM after posterior hyaloid face separation. Histologically these tissues have been comprehensively described, but how they relate to ILM-specific dye staining patterns observed during surgery is less clear.[12-14]

Also known as Coomassie Brilliant Blue G-250, BBG is a blue triphenylmethane dye with a molecular weight of 856 g/mol and the molecular formula $C_{47}H_{50}N_3NaO_7S_2$. It was first developed for use in the textile industry but then was used in biochemistry relating to its protein-binding properties.[15] Similar to ICG, BBG appears to be an ILM-specific dye, and clinically it has been observed that material overlying the ILM at the time of its application is not stained. This phenomenon has been used to facilitate double peeling of epiretinal membrane (ERM) followed by ILM.[4] The precise mechanism of its ILM specificity is unknown but may relate to the difference between the compact nature of the predominant type IV collagen in ILM compared to the more fibrillary structure of ERMs and type II collagen in native vitreous remnants, graphically seen in scanning electron microscope images of the two surfaces.[16]

We observed nonuniform staining of BBG over the macular area in 40% of our cases, with 31% of patients having discrete areas of nonstaining and 9% having more generalized and confluent zones of nonstaining around the hole. If those cases with a nonstaining rim are included, then 64% of all the patients had some area of nonstaining. This concurs with the findings of Husson-Danan et al.,[9] who noted that areas of nonstaining were visible in 61% of patients with a MH using ICG staining; however, the characteristics of the nonstaining pattern were not described further, and their relationship with preoperative hole characteristics or postoperative outcome was not investigated. The percentage of patients with nonuniform staining is in broad agreement with histologic studies of ILM specimens displaying fibrocellular material on the ILM surface. Kenawy et al.[17] found fibrocellular material on 30% of ILM specimens from macular holes, while Schumann et al.[12] described fibrocellular material in 57% of eyes. Schumann et al.[3] noted a correlation between the presence and extent of fibrocellular material and stage 4 holes and suggested that spontaneous posterior vitreous separation in MH patients is associated with greater degrees of residual vitreous adherent to the retinal surface. We found the same association, with 89% of patients with stage 4 holes having an incomplete staining pattern compared to only 24% of the patients with stage 2 holes. This was also confirmed histologically, with a mean percentage of ILM covered by vitreous "debris" of 48.9% in stage 4 holes against only 7.4% in stage 2 holes. More importantly, we were able to show a clear relationship between the presence of nonstaining areas on the ILM clinically and the amount of vitreous-side tissue present histologically, allowing us to gauge the amount of vitreous-side tissue present from the staining pattern alone. Thus in one of the stage 2 holes examined histologically, there was patchy staining with significant vitreous-side tissue present histologically, and in one of the stage 4 holes the staining pattern was

TABLE 3. Patient Characteristics Between Those With a Nonstaining Rim and Those Without

	Rim +ve, $n = 31$	Rim −ve, $n = 24$	P
Age, y, mean	69.96	70.26	0.876
Female sex (%)	21 (68)	19 (79)	0.526
Stages 2, 3, 4, %	9, 13, 4	15, 7, 5	0.210
MLD, μm, mean (range)	440.35 (130–845)	320.59 (120–850)	0.024*
Vitreous attachment present (%)	10 (33)	11 (46)	0.999
Preoperative Va, logMAR, mean	1.07	1.00	0.721
Postoperative Va, logMAR, mean	0.45	0.28	0.002†
Nonclosure, n	1	1	0.999

Rim +ve, a nonstaining rim was present around the hole; Rim −ve, the rim of the hole stained evenly.
* Effect size $r = 0.298$.
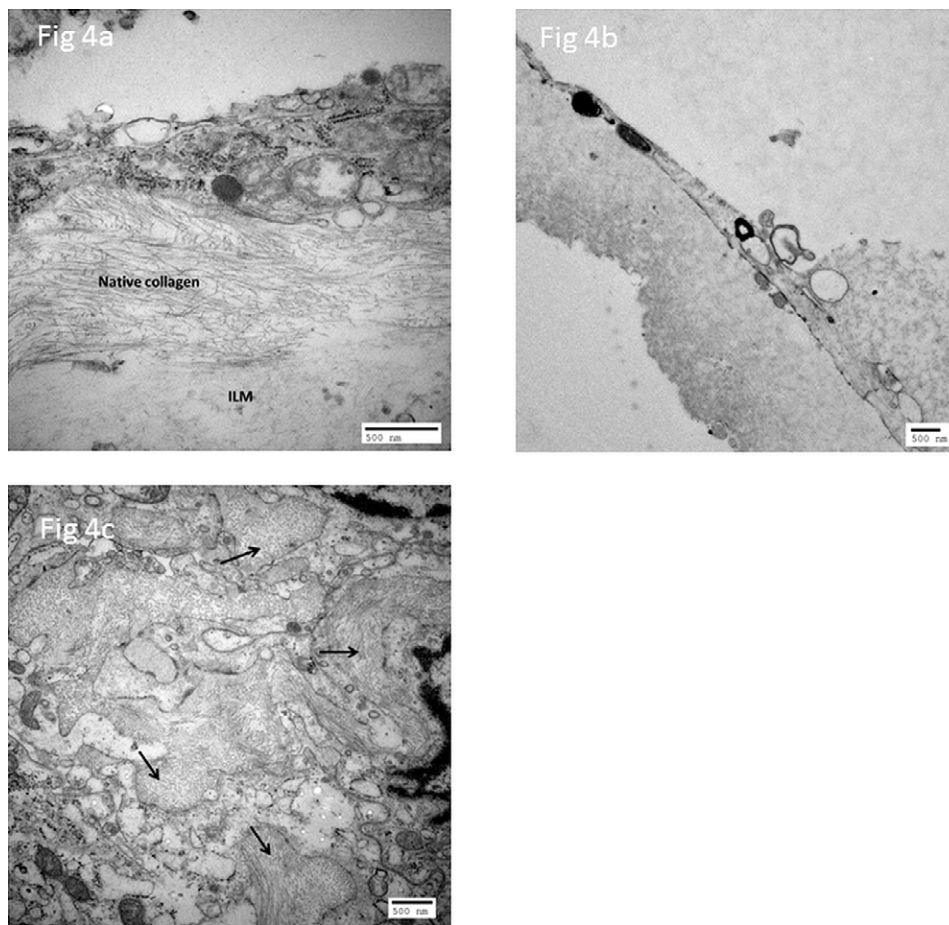† Effect size $r = 0.452$.

FIGURE 4. (a–c) Examples of the ILM vitreous-side tissue observed. (a) A multicellular membrane on a layer of intervening native vitreous collagen. (b) A monolayer of cells directly on the ILM. (c) Newly formed collagen interspersed with a multicellular layer of cells (*arrows*).

uniform with only minor amounts of vitreous-side tissue present.

The pattern of cellular debris and the presence of native and newly formed collagen varied considerably between specimens. There was no clear relationship with Gass MH stage, but there were significantly more multicellular membranes present and newly formed collagen with the incom-

plete staining patterns than in the uniform staining pattern patients.

Chang[8] noted that a nonstaining rim around the MH was visible in some cases but did not quantify its occurrence or size. We found a nonstaining rim in approximately 50% of our cases; it measured on average 291 μm in width in the uniform and patchy staining pattern groups.
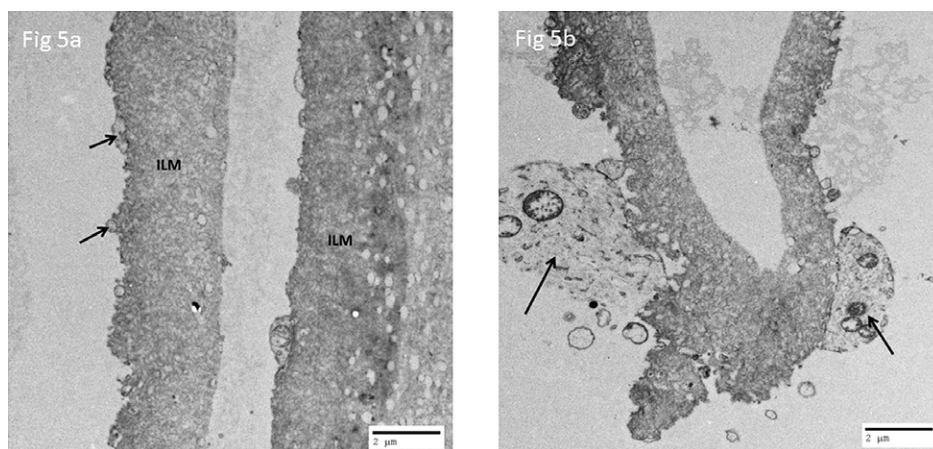

FIGURE 5. (a, b) Examples of ILM retinal-side cellular tissue. (a) Small fragments of cells on the retinal side of the ILM (arrows). (b) Larger incomplete fragments with identifiable organelles visible (*arrows*).

TABLE 4. Vitreous- and Retinal-Side Tissue Found in the Study Population

	Uniform, $n = 12$	Patchy and Nonstaining, $n = 9$	P
Vitreous-side tissue			
None	8	1	0.015
Single cells	2	1	
Monolayer of cells	1	3	
Multilayered cell sheets	1	5	
Vitreous-side collagen			
None	8	1	0.014
Native collagen	3	3	
Newly formed collagen	1	6	
Retinal-side tissue			
Small fragments	8	6	0.999
Whole cells	3	3	
Layered cells	1	0	

TABLE 6. Electron Microscopy Findings of Nonstaining Rim ILM From Three Patients

	Patient 1	Patient 2	Patient 3
Overall staining pattern	Uniform	Uniform	Uniform
Stage	3	3	2
MLD, μm	355	440	317
Mean rim radius, μm	405	425	275
Maximum rim radius, μm	420	500	410
Percent vitreous-side tissue	45	70	38
Percent retinal-side tissue	23	29	22
Type of vitreous cellular tissue	Monolayer	Monolayer	Single cells
Vitreous collagen remnants	None	None	None

Hisatomi et al.[13] described the occurrence of cellular clusters radiating away from the MH rim and related the extent to the MH stage in 23 flat-mounted ILM specimens. The nonstaining rim we observed clinically likely corresponds to the cellular clusters radiating from the hole as described by Hisatomi et al.[13] This would concur with our finding that the rim size was correlated to the MH size. The postoperative visual outcome was significantly worse in the group with a nonstaining rim. This is most likely related to the larger hole size in this group and probable longer duration of the hole, although this was not systematically recorded.[18-20]

We were able to examine the ILM confined to the rim area in three patients with a uniform staining pattern and a nonstaining rim. It is interesting that vitreous collagen was not found in any of these patients and that all had only monocellular membranes without intervening vitreous collagen present. This is in contradistinction to Hisatomi et al.[13] and Gandorfer et al.,[14] who found an intervening layer of native vitreous collagen at the rim area on their flat-mounted specimens examined with TEM. The difference may be explained by case selection. If we had examined patients with incomplete staining patterns and a nonstaining rim, we might have seen intervening collagen. Our findings mean that a layer of cells can form around the rim of a MH without any intervening vitreous collagen and be seen clinically as a nonstaining rim. Schumann et al.[12] reported that 24% of the ILMs they examined from patients with stage 3 macular holes had areas of cellular proliferation on the ILM without any intervening collagen, although they were not able to localize the areas involved. Interestingly, we did not find any association between the presence of a rim and the presence of vitreous attachment to the MH margin on the preoperative OCT.

We observed some fragments of cellular material on the retinal side of the ILM in all the ILMs examined, ranging from 12% to 45%. This has previously been shown to represent avulsed Müller cell endplates that abut onto the ILM.[21] Differing amounts of Müller cell debris have previously been found with differing stains.[22-24] Brockmann et al.[22] found higher rates of Müller cell debris with BBG than with ICG while Schumann et al.[23] found the reverse. For this reason we used only one formulation of BBG stain and standardized its application time throughout the study period. It has been suggested that ERM may be associated with sub-ILM changes that alter the plane of separation during ILM peeling.[17] We did not, however, find any association between the extent of vitreous-side tissue and retinal-side tissue in our cases. This may be related to the lesser amounts of ERM in our series without related sub-ILM changes seen in more advanced ERMs. We also investigated whether the amount of retinal hemorrhaging occurring spontaneously during ILM peeling was related to the staining pattern or amount of retinal-side tissue observed on TEM. We did not find any relationship, but this may have had to do with the sample size. The regression coefficient of approximately 0.3 between hemorrhages and retinal-side tissue suggests that there may be a significant relationship, and this would be interesting to study with larger numbers.

There are several limitations to our study. The number of cases examined with electron microscopy was relatively low, but we were able to demonstrate clear correlation between the observed staining patterns and the histologic findings. Using TEM, we were not able to precisely topographically correlate the areas of nonstaining with the histology. This could be achieved in future studies using flat-mounted specimens. It is also important to note that the findings of our study may be specific to the exact formulation of the BBG brand and the application procedure used. It is possible that differing concentrations and formulations of BBG could alter the staining patterns observed.[25]

Importantly, this study has provided a direct clinicopathologic correlation between the staining patterns of the ILM-specific dye BBG and ILM vitreous surface tissue. Inner limiting membrane peeling has been shown to improve closure rate in MH surgery. However, its use has been associated with a growing list of potential adverse effects.[26,27] It is interesting to postulate that the areas of nonstaining described, representing persistent cortical vitreous or cellular proliferation, could be used to guide the surgeon as to the extent, or even the necessity, of ILM peeling required. This is of particular interest in small holes, where the benefits of ILM peeling have been questioned.[28] For example, in a patient with a small hole and a uniform staining pattern but with a nonstaining rim, it may be

TABLE 5. Percentage of ILM Sections With Retinal- or Vitreous-Side Tissue Between the Three Staining Groups

	Uniform	Patchy	Nonstaining	P
Percent vitreous-side tissue, mean	5.23	47.29	68.00	0.0000056
Percent retinal-side debris, mean	29.0	28.57	33.00	0.819

necessary to peel the ILM only in the immediate rim area. Further studies utilizing the staining patterns of ILM-specific dyes to guide the extent of ILM peeling would be of interest.

References

1. Spiteri Cornish K, Lois N, Scott NW, et al. Vitrectomy with internal limiting membrane peeling versus no peeling for idiopathic full-thickness macular hole. *Ophthalmology*. 2014; 121:649–655.

2. Shimada H, Nakashizuka H, Hattori T, Mori R, Mizutani Y, Yuzawa M. Double staining with brilliant blue G and double peeling for epiretinal membranes. *Ophthalmology*. 2009;116: 1370–1376.

3. Schumann RG, Gandorfer A, Eibl KH, Henrich PB, Kampik A, Haritoglou C. Sequential epiretinal membrane removal with internal limiting membrane peeling in brilliant blue G-assisted macular surgery. *Br J Ophthalmol*. 2010;94:1369–1372.

4. Enaida H, Hisatomi T, Hata Y, et al. Brilliant blue G selectively stains the internal limiting membrane/brilliant blue G-assisted membrane peeling. *Retina*. 2006;26:631–636.

5. Remy M, Thaler S, Schumann RG, et al. An in vivo evaluation of Brilliant Blue G in animals and humans. *Br J Ophthalmol*. 2008;92:1142–1147.

6. Eshita T, Ishida S, Shinoda K, et al. Indocyanine green can distinguish posterior vitreous cortex from internal limiting membrane during vitrectomy with removal of epiretinal membrane. *Retina*. 2002;22:104–106.

7. Gandorfer A, Messmer EM, Ulbig MW, Kampik A. Indocyanine green selectively stains the internal limiting membrane. *Am J Ophthalmol*. 2001;131:387–388.

8. Chang S. Controversies regarding internal limiting membrane peeling in idiopathic epiretinal membrane and macular hole. *Retina*. 2012;32(suppl 2):S200–S203.

9. Husson-Danan A, Glacet-Bernard A, Soubrane G, Coscas G. Clinical evaluation of the use of indocyanine green for peeling the internal limiting membrane in macular hole surgery. *Graefes Arch Clin Exp Ophthalmol*. 2006;244:291–297.

10. DeCroos FC, Toth CA, Folgar FA, et al. Characterization of vitreoretinal interface disorders using OCT in the interventional phase 3 trials of ocriplasmin. *Invest Ophthalmol Vis Sci*. 2012;53:6504–6511.

11. Gass JD. Reappraisal of biomicroscopic classification of stages of development of a macular hole. *Am J Ophthalmol*. 1995; 119:752–759.

12. Schumann RG, Schaumberger MM, Rohleder M, Haritoglou C, Kampik A, Gandorfer A. Ultrastructure of the vitreomacular interface in full-thickness idiopathic macular holes: a consecutive analysis of 100 cases. *Am J Ophthalmol*. 2006;141:1112– 1119.

13. Hisatomi T, Enaida H, Sakamoto T, et al. Cellular migration associated with macular hole: a new method for comprehen-

14. Gandorfer A, Scheler R, Haritoglou C, Schumann R, Nentwich M, Kampik A. Pathology of the macular hole rim in flat-mounted internal limiting membrane specimens. *Retina*. 2009;29:1097–1105.

15. Coomassie Brilliant Blue. Available at: http://en.wikipedia.org/wiki/Coomassie_Brilliant_Blue. Accessed August 1, 2014.

16. Gandorfer A, Ulbig M, Kampik A. Plasmin-assisted vitrectomy eliminates cortical vitreous remnants. *Eye (Lond)*. 2002;16: 95–97.

17. Kenawy N, Wong D, Stappler T, et al. Does the presence of an epiretinal membrane alter the cleavage plane during internal limiting membrane peeling? *Ophthalmology*. 2010;117:320– 323.

18. Ullrich S, Haritoglou C, Gass C, Schaumberger M, Ulbig MW, Kampik A. Macular hole size as a prognostic factor in macular hole surgery. *Br J Ophthalmol*. 2002;86:390–393.

19. Gupta B, Laidlaw DA, Williamson TH, Shah SP, Wong R, Wren S. Predicting visual success in macular hole surgery. *Br J Ophthalmol*. 2009;93:1488–1491.

20. Wakely L, Rahman R, Stephenson J. A comparison of several methods of macular hole measurement using optical coherence tomography, and their value in predicting anatomical and visual outcomes. *Br J Ophthalmol*. 2012;96:1003–1007.

21. Wolf S, Schnurbusch U, Wiedemann P, Grosche J, Reichenbach A, Wolburg H. Peeling of the basal membrane in the human retina: ultrastructural effects. *Ophthalmology*. 2004;111:238– 243.

22. Brockmann T, Steger C, Westermann M, et al. Ultrastructure of the membrana limitans interna after dye-assisted membrane peeling. *Ophthalmologica*. 2011;226:228–233.

23. Schumann RG, Gandorfer A, Priglinger SG, Kampik A, Haritoglou C. Vital dyes for macular surgery: a comparative electron microscopy study of the internal limiting membrane. *Retina*. 2009;29:669–676.

24. Konstantinidis L, Uffer S, Bovey EH. Ultrastructural changes of the internal limiting membrane removed during indocyanine green assisted peeling versus conventional surgery for idiopathic macular epiretinal membrane. *Retina*. 2009;29: 380–386.

25. Uemoto R, Nakasato-Sonn H, Meguro A, Ito N, Yazama F, Mizuki N. Staining internal limiting membrane with a mixture of BBG and sodium hyaluronate. *Br J Ophthalmol*. 2013;97: 690–693.

26. Pichi F, Lembo A, Morara M, et al. Early and late inner retinal changes after inner limiting membrane peeling. *Int Ophthalmol*. 2014;34:437–446.

27. Tadayoni R, Paques M, Massin P, et al. Dissociated optic nerve fiber layer appearance of the fundus after idiopathic epiretinal membrane removal. *Ophthalmology*. 2001;108:2279–2283.

28. Tadayoni R, Gaudric A, Haouchine B, Massin P. Relationship between macular hole size and the potential benefit of internal limiting membrane peeling. *Br J Ophthalmol*. 2006;90:1239– 1241.